IL NUOVO CIMENTO Vol. 34 C, N. 5 Suppl. 1 Settembre-Ottobre 2011
DOI 10.1393/ncc/i2011-10999-1

Colloquia: LC10

Probing supersymmetry with flavour physics data

F. Mahmoudi

CERN Theory Division, Physics Department - CH-1211 Geneva 23, Switzerland
Clermont Université, Université Blaise Pascal, CNRS/IN2P3
LPC, BP 10448, 63000 Clermont-Ferrand, France

(ricevuto il 20 Luglio 2011; pubblicato online il 6 Ottobre 2011)

Summary. — An overview of the indirect constraints from flavour physics on supersymmetric models is presented. During the past few years flavour data, and in particular $b \to s\gamma$ transitions, have been extensively used in order to constrain supersymmetric parameter spaces. We will briefly illustrate here the constraints obtained by a collection of low energy observables including, rare decays, leptonic and semileptonic decays of B mesons, as well as leptonic decays of K and D_s mesons. The SuperIso program which is dedicated to flavour physics observable calculations is also described briefly.

PACS 11.30.Pb – Supersymmetry.
PACS 13.20.-v – Leptonic, semileptonic, and radiative decays of mesons.

1. – Introduction

In addition to direct searches for new physics and new effects, indirect searches play an important and complementary role in the quest for physics beyond the Standard Model (SM). The most commonly used indirect constraints originate from flavour physics observables, cosmological data and relic density, electroweak precision tests and anomalous magnetic moment of the muon. Precise experimental measurements and theoretical predictions have been achieved for the B meson systems in the past decade [1] and stringent constraints due to sizeable new physics contributions to many observables can be obtained [2-4]. In the following, we present an overview of the most constraining flavour physics observables, namely the branching ratios of $B \to X_s\gamma$, $B_s \to \mu^+\mu^-$, $B \to X_s\mu^+\mu^-$, $B \to \tau\nu_\tau$, $B \to D\tau\nu_\tau$ as well as $D_s \to \tau\nu_\tau$ and $K \to \mu\nu_\mu$. For each observable we determine the regions excluded in the MSSM parameter space. In the constrained MSSM scenarios, such as CMSSM or NUHM which we investigate here, the fact that the number of free parameters is drastically reduced as compared to the general MSSM allows for the observables to probe deeply the structure of the model. This indirect information, in addition to the direct searches for new physics, will be very useful for the physics strategy of a future linear collider.

TABLE I. – *Input parameters (in GeV if not specified otherwise)* [6].

m_π	m_K	m_{K^*}	m_{D^0}	m_D	m_{D_s}	m_B	m_{B_s}
0.1396	0.4937	0.8917	1.8648	1.8696	1.9685	5.2792	5.3663

$\overline{m}_b(\overline{m}_b)$	$\overline{m}_c(\overline{m}_c)$	m_s	$m_t^{\rm pole}$	$\alpha_s(M_Z)$
$4.19^{+0.18}_{-0.06}$	$1.27^{+0.07}_{-0.09}$	$0.101^{+0.029}_{-0.021}$	173.3 ± 1.1	0.1184 ± 0.0008

f_K/f_π	f_{K^*} (MeV)	f_B (MeV)	λ_B (MeV)	f_{B_s} (MeV)	f_{D_s} (MeV)
1.193 ± 0.006	220 ± 5	192.8 ± 9.9	510 ± 120	238.8 ± 9.5	248 ± 2.5

$\lvert V_{ud}\rvert$	$\lvert V_{us}\rvert$	$\lvert V_{ub}\rvert$	$\lvert V_{cs}\rvert$
0.97428 ± 0.00015	0.2253 ± 0.0007	$(3.92 \pm 0.46)\,10^{-3}$	0.97345 ± 0.00016

$\lvert V_{cb}\rvert$	$\lvert V_{td}\rvert$	$\lvert V_{ts}\rvert$	$\lvert V_{tb}\rvert$
$(4.10 \pm 0.11) \times 10^{-2}$	$(8.62 \pm 0.26) \times 10^{-3}$	$(4.03 \pm 0.11) \times 10^{-2}$	0.999152 ± 0.000045

C	E_0	λ_2 (GeV^2)	BR$(B \to X_c e \bar{\nu})_{\rm exp}$
0.58 ± 0.01	1.6	0.12	0.1061 ± 0.0017

All the observables presented here are calculated with the publicly available program SuperIso [5-7]. A brief description of each observable is provided below, and a more detailed description of the calculations can be found in [6]. The input parameters used in the following calculations are given in table I.

2. – Flavour physics constraints

Flavour observables can be classified in different categories, such as radiative penguin decays, electroweak penguin decays, neutrino modes and meson mixings.

The inclusive branching ratio of $B \to X_s\gamma$ and the isospin asymmetry of $B \to K^*\gamma$ are the most important observables in the first category. Since $b \to s\gamma$ transition occurs first at one-loop level in the SM, new physics contributions can be of comparable magnitude. Here penguin loops involve the W boson in the Standard Model, and in addition charged Higgs boson, chargino, neutralino and gluino in the MSSM. The charged Higgs loop always adds constructively to the SM penguin. Thus, BR$(B \to X_s\gamma)$ is an effective tool to probe the THDM scenario. Chargino loops however can add constructively or destructively. If the interference is positive, it results in a great enhancement in the BR$(B \to X_s\gamma)$, which becomes therefore a powerful observable. On the other hand, if the interference is negative, the other interesting observable which opens up is the degree of isospin asymmetry in the exclusive decay of $B \to K^*\gamma$.

The latest combined experimental value for BR$(B \to X_s\gamma)$ is reported by the Heavy Flavor Averaging Group (HFAG) [8]:

$$\text{BR}(\bar{B} \to X_s\gamma)^{\rm exp} = (3.55 \pm 0.24 \pm 0.09) \times 10^{-4}. \tag{1}$$

Following [9, 10], we calculate this branching ratio at the NNLO accuracy. With the most up-to-date parametric inputs as given in [11] the SM prediction reads([1])

$$\mathrm{BR}(\bar{B} \to X_s\gamma)^{\mathrm{SM}} = (3.09 \pm 0.22) \times 10^{-4}. \tag{2}$$

The allowed range at 95% CL for this branching ratio, including both the theoretical and experimental uncertainties is [6]

$$2.16 \times 10^{-4} \leq \mathrm{BR}(\bar{B} \to X_s\gamma) \leq 4.93 \times 10^{-4}. \tag{3}$$

To investigate the NUHM parameter space, we perform scans over the parameters such that $m_0 \in [50, 2000]\,\mathrm{GeV}$, $m_{1/2} \in [50, 2000]\,\mathrm{GeV}$, $A_0 \in [-2000, 2000]\,\mathrm{GeV}$, $\mu \in [0, 2000]\,\mathrm{GeV}$, $m_A \in [5, 600]\,\mathrm{GeV}$ and $\tan\beta \in [1, 60]$. Figure 1(a) shows the resulting constraints projected in the $(m_{H^+}, \tan\beta)$-plane. The excluded points are shown in red and the allowed points are displayed in green in the foreground.

While in the CMSSM the isospin asymmetry of $B \to K^*\gamma$ appears to be very constraining [12], in NUHM since m_{H^+} can be treated as a free parameter, it is easier to evade this constraint by adjusting the parameters.

The most relevant observables in electroweak penguin decays are the branching ratio of $B_s \to \mu^+\mu^-$, branching ratios and forward-backward asymmetries in $B \to X_s\,\mu^+\mu^-$ and $B \to K^{(*)}\mu^+\mu^-$ decays. The current experimental limit for $\mathrm{BR}(B_s \to \mu^+\mu^-)$, derived by the CDF Collaboration at 95% CL, is [13]

$$\mathrm{BR}(B_s \to \mu^+\mu^-) < 4.3 \times 10^{-8}. \tag{4}$$

In supersymmetry, for large values of $\tan\beta$, this decay can receive large contributions from neutral Higgs bosons. Including theoretical uncertainties, we compare the MSSM prediction to the upper limit at 95% CL

$$\mathrm{BR}(B_s \to \mu^+\mu^-) < 6.6 \times 10^{-8}, \tag{5}$$

in order to explore the constraints imposed by this observable. The results are illustrated in fig. 1(b). In the same way, we can use the latest Belle and Babar results for $\mathrm{BR}(B \to X_s\mu^+\mu^-)$, separately for high and low q^2 regimes [11]:

$$\mathrm{BR}(B \to X_s\mu^+\mu^-) = (1.6 \pm 0.5) \times 10^{-6}, \qquad 1 < q^2 < 6\,\mathrm{GeV}^2, \tag{6}$$

$$\mathrm{BR}(B \to X_s\mu^+\mu^-) = (4.4 \pm 1.3) \times 10^{-7}, \qquad q^2 > 14.4\,\mathrm{GeV}^2, \tag{7}$$

leading to the following allowed intervals at 95% CL:

$$0.6 \times 10^{-6} < \mathrm{BR}(B \to X_s\mu^+\mu^-) < 2.6 \times 10^{-6}, \qquad 1 < q^2 < 6\,\mathrm{GeV}^2, \tag{8}$$

$$1.8 \times 10^{-7} < \mathrm{BR}(B \to X_s\mu^+\mu^-) < 7.0 \times 10^{-7}, \qquad q^2 > 14.4\,\mathrm{GeV}^2. \tag{9}$$

The results are presented in figs. 1(c) and (d). It is important to remember that using the upcoming LHCb results, various observables corresponding to $b \to s\mu^+\mu^-$ transitions would provide very restrictive constraints in the near future.

([1]) The slight difference compared to earlier published results is explained by the parametric updates.

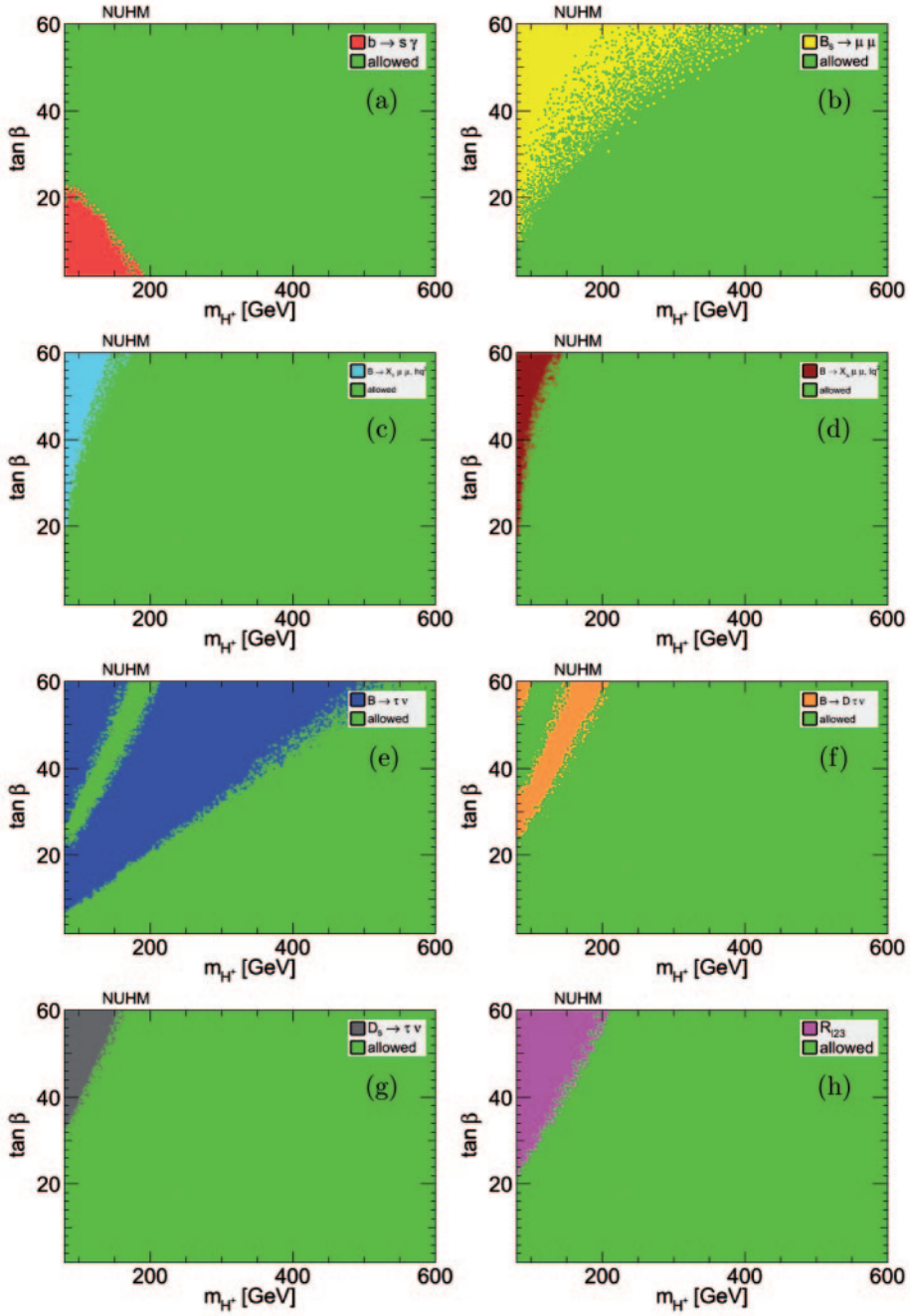

Fig. 1. – (Colour on-line) Constraints on the NUHM parameter plane $(m_{H^+}, \tan\beta)$ from the branching ratios of $b \to s\gamma$ (red), $B_s \to \mu^+\mu^-$ (yellow), $B \to X_s\mu^+\mu^-$ at low q^2 (light blue), $B \to X_s\mu^+\mu^-$ at high q^2 (dark red), $B_u \to \tau\nu_\tau$ (blue), $B \to D\tau\nu_\tau$ (orange), $D_s \to \tau\nu_\tau$ (grey) and $K \to \mu\nu_\mu$ (magenta). The allowed points are displayed in the foreground.

Finally in the neutrino mode category, branching ratios of $B_u \to \tau\nu_\tau$, $B \to D\tau\nu_\tau$, $D_s \to \tau\nu_\tau$, $D_s \to \mu\nu_\mu$, $K \to \mu\nu_\mu$, as well as double ratios of leptonic decays are the most important observables. These decays can be mediated by a charged Higgs boson already at tree level in annihilation processes and therefore are very sensitive to the charged Higgs sector. The current HFAG value for $\mathrm{BR}(B_u \to \tau\nu_\tau)$ is [8]

$$\mathrm{BR}(B_u \to \tau\nu_\tau)^{\mathrm{exp}} = (1.64 \pm 0.34) \times 10^{-4}. \tag{10}$$

The evaluation of $\mathrm{BR}(B_u \to \tau\nu_\tau)$ suffers however from the uncertainties in the determination of $|V_{ub}|$. We consider the following ratio to express the new physics contributions:

$$R_{\tau\nu_\tau} = \frac{\mathrm{BR}(B_u \to \tau\nu_\tau)^{\mathrm{NP}}}{\mathrm{BR}(B_u \to \tau\nu_\tau)^{\mathrm{SM}}} = \left[1 - \left(\frac{m_B^2}{M_{H^+}^2}\right) \frac{\tan^2\beta}{1 + \epsilon_0 \tan\beta}\right]^2. \tag{11}$$

In the SM, $R_{\tau\nu_\tau}^{\mathrm{SM}} = 1$. The experimental result for this ratio is [8]

$$R_{\tau\nu_\tau}^{\mathrm{exp}} = 1.63 \pm 0.54, \tag{12}$$

leading to the following allowed interval at 95% CL [6]:

$$0.56 < R_{\tau\nu_\tau} < 2.70. \tag{13}$$

The resulting constraints are shown in fig. 1(e).

The semileptonic decays $B \to D\ell\nu$ [14] have the advantage of depending on $|V_{cb}|$, which is known to better precision than $|V_{ub}|$. In addition, the $\mathrm{BR}(B \to D\tau\nu_\tau)$ is about 50 times larger than $\mathrm{BR}(B_u \to \tau\nu_\tau)$ in the SM. Due to the presence of at least two neutrinos in the final state, the experimental determination remains however very complex. To reduce some of the theoretical uncertainties, we consider the following ratio:

$$\xi_{D\ell\nu} \equiv \frac{\mathrm{BR}(B \to D\tau\nu_\tau)}{\mathrm{BR}(B \to De\nu_e)}. \tag{14}$$

The SM prediction for this ratio is [6]

$$\xi_{D\ell\nu}^{\mathrm{SM}} = (29 \pm 3) \times 10^{-2}, \tag{15}$$

and the experimental result by the BaBar Collaboration reads [15]

$$\xi_{D\ell\nu}^{\mathrm{exp}} = (41.6 \pm 11.7 \pm 5.2) \times 10^{-2}. \tag{16}$$

The 95% CL allowed interval is given by [6]

$$0.151 < \xi_{D\ell\nu} < 0.681, \tag{17}$$

leading to the constraints shown in fig. 1(f).

In analogy to the case for $B_u \to \tau\nu_\tau$, charged Higgs bosons would also contribute to the decays $D_s \to \tau\nu_\tau$ at tree level [16]. The experimental results for this branching ratio is [8,17]

$$\mathrm{BR}(D_s \to \tau\nu_\tau)^{\mathrm{exp}} = (5.38 \pm 0.32) \times 10^{-2}, \tag{18}$$

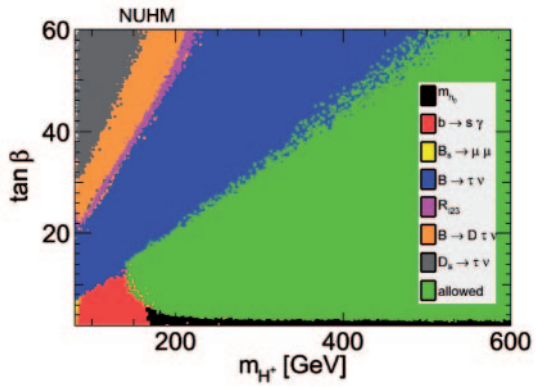

Fig. 2. – (Colour on-line) Combined exclusion in NUHM models by different constraints. The constraints are applied in the order they appear in the legend, and the colour coding corresponds to the first constraint by which a point is excluded. All points have $\mu > 0$ and a neutral LSP.

while the SM prediction reads [6]

$$\mathrm{BR}(D_s \to \tau\nu_\tau)^{\mathrm{SM}} = (5.10 \pm 0.13) \times 10^{-2}. \tag{19}$$

We consider the following allowed interval at 95% CL [6]:

$$4.7 \times 10^{-2} < \mathrm{BR}(D_s \to \tau\nu_\tau) < 6.1 \times 10^{-2}, \tag{20}$$

and the results are shown in fig. 1(g).

The last leptonic decay that we consider is the decay $K \to \mu\nu_\mu$, and in particular we consider the ratio [18]

$$R_{\ell 23} = \left|\frac{V_{us}(K_{\ell 2})}{V_{us}(K_{\ell 3})} \times \frac{V_{ud}(0^+ \to 0^+)}{V_{ud}(\pi_{\ell 2})}\right| = \left|1 - \frac{m_{K^+}^2}{M_{H^+}^2}\left(1 - \frac{m_d}{m_s}\right)\frac{\tan^2\beta}{1 + \epsilon_0 \tan\beta}\right|. \tag{21}$$

The SM value for this ratio is $R_{\ell 23}^{\mathrm{SM}} = 1$ while the experimental measurement gives [18]

$$R_{\ell 23}^{\mathrm{exp}} = 0.999 \pm 0.007, \tag{22}$$

and the allowed interval at 95% CL reads

$$0.985 < R_{\ell 23} < 1.013, \tag{23}$$

resulting in the constraints displayed in fig. 1(h).

Figure 2 shows a combination of constraints applied to the NUHM parameter space [3]. Here we see that charged Higgs masses down to $m_{H^+} \simeq 135\,\mathrm{GeV}$ can be accommodated, with the lowest masses allowed for intermediate $\tan\beta \sim 7$–15. For higher $\tan\beta$, the combined constraints follow the exclusion by $B_u \to \tau\nu_\tau$. This figure illustrates that most of the indirect constraints are relevant in the same parameter space regions where the charged Higgs production cross section at the LHC is the largest. An early discovery of

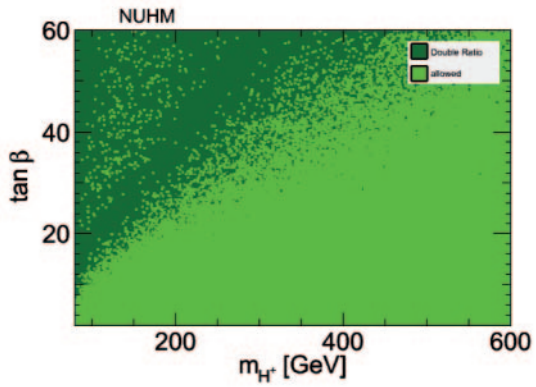

Fig. 3. – (Colour on-line) Constraints obtained by the double ratio R in the NUHM plane $(m_{H^+}, \tan\beta)$. The zones in dark green are excluded at 95% CL.

the charged Higgs would therefore serve as an indication of a non-minimal model being realized in nature.

Most of the leptonic observables are subject to uncertainties from decay constants. In order to remove such uncertainties it is possible to define double ratios of leptonic decays in a way to cancel the dependency on the decay constants [19, 20]. We consider the constraints obtained by the following double ratio [20]:

$$R = \left(\frac{\mathrm{BR}(B_s \to \mu^+\mu^-)}{\mathrm{BR}(B_u \to \tau\nu_\tau)}\right) \Big/ \left(\frac{\mathrm{BR}(D_s \to \tau\nu_\tau)}{\mathrm{BR}(D \to \mu\nu_\mu)}\right). \tag{24}$$

The results are shown in the plane $(m_{H^+}, \tan\beta)$ in fig. 3, where the dark green points, displayed in the background, are excluded by R. In a large part of the parameter space, the double ratio is SM-like. In these regions, one can obtain $|V_{ub}|$ once the four decays involved in eq. (24) are measured with almost no additional deviation due to SUSY. On the other hand, one can use $|V_{ub}|$ as an input parameter and in this case as can be seen from the figure, the area with $m_{H^+}/\tan\beta < 8\,\mathrm{GeV}$ is excluded with no dependence on the lattice inputs.

3. – SuperIso program

SuperIso [5-7] is a public C program dedicated mostly to the calculation of flavour physics observables. The calculations are done in various models, such as SM, THDM, MSSM and NMSSM with minimal flavour violation. A broad set of flavour physics observables is implemented in SuperIso. This includes the branching ratio of $B \to X_s\gamma$, isospin asymmetry of $B \to K^*\gamma$, branching ratio of $B_s \to \mu^+\mu^-$, branching ratios of $B_s \to X_s\mu^+\mu^-$, $B_s \to K^*\mu^+\mu^-$, $B_s \to K\mu^+\mu^-$ and the forward backward asymmetries in these decays, branching ratio of $B_u \to \tau\nu_\tau$, branching ratio of $B \to D\tau\nu_\tau$, branching ratio of $K \to \mu\nu_\mu$, branching ratio of $D \to \mu\nu_\mu$, and the branching ratios of $D_s \to \tau\nu_\tau$ and $D_s \to \mu\nu_\mu$. The calculation of the anomalous magnetic moment of the muon is also implemented in the program. SuperIso uses a SUSY Les Houches Accord (SLHA) file [21] as input, which can be either generated automatically by the program via a call

to a spectrum generator or provided by the user. The program is able to perform the calculations automatically for different SUSY breaking scenarios. An extension of SuperIso including the relic density calculation, SuperIso Relic, is also available publicly [22]. Finally, in SuperIso we make use of the Flavour Les Houches Accord (FLHA) [23], the newly developed standard for flavour related quantities, and the program provides an FLHA output file as well.

4. – Conclusion

Indirect constraints and in particular those from flavour physics are essential to restrict new physics parameters as we have seen here. The information obtained from these low energy observables combined with the collider data will open the door to a very rich phenomenology and would help us advance toward a deeper understanding of the governing physics. This information will also be very valuable in the design and search strategy of a future linear collider. Here we showed a few examples of possible analyses but the same methods can of course be generalized to more new physics scenarios.

REFERENCES

[1] For a recent review see: Hurth T. and Nakao M., *Annu. Rev. Nucl. Part. Sci.*, **60** (2010) 645 [arXiv:1005.1224].
[2] See for example: Carena M. S. *et al.*, *Phys. Rev. D*, **74** (2006) 015009 [hep-ph/0603106]; Ellis J. R., Heinemeyer S., Olive K. A. and Weiglein G., *Phys. Lett. B*, **653** (2007) 292 [arXiv:0706.0977]; Mahmoudi F., *JHEP*, **0712** (2007) 026 [arXiv:0710.3791].
[3] Eriksson D., Mahmoudi F. and Stål O., *JHEP*, **0811** (2008) 035 [arXiv:0808.3551].
[4] Mahmoudi F. and Stål O., *Phys. Rev. D*, **81** (2010) 035016 [arXiv:0907.1791].
[5] Mahmoudi F., *Comput. Phys. Commun.*, **178** (2008) 745 [arXiv:0710.2067].
[6] Mahmoudi F., *Comput. Phys. Commun.*, **180** (2009) 1579 [arXiv:0808.3144].
[7] Mahmoudi F., *Comput. Phys. Commun.*, **180** (2009) 1718, `http://superiso.in2p3.fr`.
[8] Barberio E. *et al.* (Heavy Flavor Averaging Group), arXiv:0808.1297 [hep-ex], and online update at `http://www.slac.stanford.edu/xorg/hfag`.
[9] Misiak M. *et al.*, *Phys. Rev. Lett.*, **98** (2007) 022002 [hep-ph/0609232].
[10] Misiak M. and Steinhauser M., *Nucl. Phys. B*, **764** (2007) 62 [hep-ph/0609241].
[11] Nakamura K. (Particle Data Group), *J. Phys. G*, **37** (2010) 075021.
[12] Ahmady M. R. and Mahmoudi F., *Phys. Rev. D*, **75** (2007) 015007 [hep-ph/0608212].
[13] CDF Collaboration, CDF Public Note 9892.
[14] Grzadkowski B. and Hou W. S., *Phys. Lett. B*, **272** (1991) 383; Nierste U., Trine S. and Westhoff S., *Phys. Rev. D*, **78** (2008) 015006 [arXiv:0801.4938]; Kamenik J. F. and Mescia F., *Phys. Rev. D*, **78** (2008) 014003 [arXiv:0802.3790].
[15] Aubert B. *et al.* (BABAR Collaboration), *Phys. Rev. Lett.*, **100** (2008) 021801.
[16] Hou W. S., *Phys. Rev. D*, **48** (1993) 2342; Hewett J. L., hep-ph/9505246; Akeroyd A. G., *Prog. Theor. Phys.*, **111** (2004) 295 [hep-ph/0308260]; Akeroyd A. G. and Chen C. H., *Phys. Rev. D*, **75** (2007) 075004 [hep-ph/0701078].
[17] Akeroyd A. G. and Mahmoudi F., *JHEP*, **0904** (2009) 121 [arXiv:0902.2393].
[18] Antonelli M. *et al.*, *Eur. Phys. J. C*, **69** (2010) 399 [arXiv:1005.2323].
[19] Grinstein B., *Phys. Rev. Lett.*, **71** (1993) 3067 [hep-ph/9308226].
[20] Akeroyd A. G. and Mahmoudi F., *JHEP*, **1010** (2010) 038 [arXiv:1007.2757].
[21] P. Skands *et al.*, *JHEP*, **0407** (2004) 036 [hep-ph/0311123]; Allanach B. C. *et al.*, *Comput. Phys. Commun.*, **180** (2009) 8 [arXiv:0801.0045].
[22] Arbey A. and Mahmoudi F., *Comput. Phys. Commun.*, **181** (2010) 1277 [arXiv:0906.0369]; **182** (2011) 1582.
[23] Mahmoudi F. *et al.*, arXiv:1008.0762 [hep-ph].